Meteorological and Chemical Behavior of Gaseous Sulfur Compounds in and around an Urban Valley

Sang-Keun Song[1], Yoo-Keun Kim[1, *], and Zang-Ho Shon[2]

[1] *Division of Earth Environmental System, Pusan National University, Busan, Republic of Korea*
[2] *Department of Environmental Engineering, Dong-Eui University, Busan, Republic of Korea*

ABSTRACT

The effects of photochemical oxidation of reduced sulfur compounds (RSCs: H_2S, CH_3SH, DMS, and DMDS) on SO_2 production were evaluated at high (HV) and low ventilation (LV) conditions, based on a CALPUFF dispersion model coupled with photo-chemical oxidation mechanisms for four RSCs. The RSC emission concentrations used in the modeling were measured in and around an urban valley during a field campaign held in October 2008. SO_2 production with LV (up to 156 ppb at 0900 LST) was found to be significantly higher than that with HV (up to 30 ppb). SO_2 produced by photochemical oxidation of RSCs with LV (78% of total SO_2 concentrations) was much higher than that with HV (27%), while the predominant RSC species were similar: DMDS ($\geq 60\%$ of the total contributions) with HV and LV when compared to three other RSCs ($< 20\%$). The difference in SO_2 concentration between HV and LV might be caused by the combined effects of photochemical oxidation of RSCs and ventilation condition.

1. INTRODUCTION

Air pollutants such as methane (CH_4), reduced sulfur compounds (RSCs), and volatile organic compounds (VOCs) are known to constitute large portions of trace gas emissions in industrialized and/or polluted urban areas (Blaha et al. 1999; Watts 2000; Ito et al. 2001; Gurjar et al. 2004; Kim 2006; Warneke et al. 2007). For instance, anthropogenic CH_4 emission (e.g., 0.6 Tg yr^{-1}) in New England was estimated to be 1.5 times higher than its natural emission (e.g., 0.4)(Blaha et al. 1999). Anthropogenic emissions of major RSCs such as hydrogen sulfide (H_2S) and carbon disulfide (CS_2) in polluted urban areas (3.3 and 0.34 Tg yr^{-1}, respectively) were also significantly (up to 8 times) higher than natural emissions [in wetlands/marshes (e.g., 0.7 and 0.1 Tg yr^{-1}, respectively) and vegetation (e.g., 0.4 Tg yr^{-1})] (Watts 2000 and references therein). In addition, the anthropogenic emission rate of dimethyl sulfide (CH_3SCH_3, DMS)(0.13 Tg yr^{-1}) was similar to emission rates in marshes

(about 0.1) and wetlands (0.12), but significantly lower than emissions from vegetation (1.6)(Watts 2000). Global anthropogenic sulfur emissions (55 - 80 Tg yr^{-1})(Smith et al. 2001; Stern 2006) were estimated to be up to 3 times higher than its natural emission (25)(Bates et al. 1992). Thus, many studies in recent decades have been concerned with assessing the emission characteristics of pollutant gases under diverse environmental settings (Loizidou and Kapetanios 1992; Davoli et al. 2003; Muezzinoglu 2003; Kim 2006; Kim et al. 2006).

In general, air pollutants (and/or RSCs) released from various urban emission sources are transported to nearby dwellings and communities, and thus can lead to serious air pollution problems, and are affected by meteorological conditions and geographical features (Berman et al. 1999; Athanassiadis et al. 2002; Wargocki et al. 2002). For example, ventilation affects ozone (O_3) accumulation in the northeastern United States (Berman et al. 1999). On high-O_3 episode days, the ventilation rate during the early morning hours was nearly 50% lower than that on non-episode days. Under a high-pressure system with low and/or closed

* Corresponding author
  E-mail: kimyk@pusan.ac.kr

ventilations, high concentrations (about 120 ppb) of air pollutants (e.g., O_3) occurred in downtown Philadelphia, Pennsylvania in July 1999 (Athanassiadis et al. 2002). Some previous reports on the dispersion of odorous pollutants such as RSCs and their impact on air quality in downwind regions are available (Mussio et al. 2001; Lin et al. 2006; Song et al. 2008, 2009a). The maximum concentration of livestock odor plumes [50 odor unit (OU) m^{-3}] accumulated by windbreaks was found to be about three times higher than that induced by their dispersion without the windbreak (16 OU m^{-3})(Lin et al. 2006). In eastern Korea, a mean SO_2 concentration due to dispersion and photochemical oxidation of RSCs (a mean of 390 g hr^{-1}) and/or SO_2 (6990 g hr^{-1}) emitted from anthropogenic sources was found to be up to 1.3 times higher than that due to the natural RSC emission (10.3 g hr^{-1}) together with the same SO_2 emission (Song et al. 2009a). Although measurement techniques and modeling approaches have recently improved, they have not yet taken into consideration both the accumulation of RSCs under different ventilation conditions and chemical transformations of RSCs in urban environments.

The objective of this study was to assess the effects of photochemical oxidation of RSCs and ventilation of RSCs and SO_2 on the concentration of SO_2 in and around an urban valley. The analyses were performed based on a numerical modeling approach using data of RSC emission concentrations measured from several industrial source regions during the study period in 2008. The relative contribution of photochemical oxidation of RSCs to SO_2 concentration levels in the source regions under different ventilation conditions was also compared.

2. MATERIALS AND METHODS

2.1 Study Area and Sampling

Yangsan city, the target area in this study, includes a valley area encompassing a number of industrial facilities, public buildings, and nearby residential areas (Fig. 1). Since the early 2000s, Yangsan city has rapidly become urbanized and industrialized, causing a substantial increase in the concentration of odorous pollutants due to large point sources, geographical features (e.g., semi-closed topography), and meteorological conditions (e.g., dispersion)(Song et al. 2009b). It also includes a variety of source regions such as the industrial complexes (ICs) of Eogok (EG IC), Sanmak (SM IC), Yangsan (YS IC), and Bukjeong IC (BJ IC) located around an urban center area of Yangsan; Ungsang (US IC) and Ungbi IC (UB IC) located in the Ungsang area (the northeastern part of the study area)(Fig. 1).

In order to predict RSC behavior in the study area, emission concentrations of four RSCs were used as the input data for the numerical modeling. The RSCs measured in this study were H_2S, DMS, methyl mercaptan (CH_3SH), and dimethyl disulfide (CH_3SSCH_3, DMDS). Air samples

for the RSCs in eight sampling locations (S1 - S8), which are industrial source regions, were collected using a vacuum sampling system to fill a polyester aluminum bag (PAB) on 21 October 2008. The concentrations of RSCs were determined using a GC (GC-17A, Shimadzu Corp., Japan) with a flame photometric detector (FPD)(Song et al. 2009b). The eight sampling locations were: S1 - S3, in tire plants (0.5 km away from EG IC); S4, in a waste water disposal plant (nearly 4 km south of EG IC); S5, in a oil refinery (located between SM and BJ ICs); S6, in a paper mill/incineration plant (a circumferential area of US IC); and S7 - S8, in livestock feedlots (located between US and UB ICs)(Fig. 1). The RSC measurements were made on a once-per-day basis in the afternoon (13:10 - 16:20) for sites S1 - S5 and in the morning (09:00 - 11:10) for sites S6 - S8 during the study. Note that the sampling time was separated into two periods (morning and afternoon) during the measurement day to simultaneously investigate the meteorological and chemical behavior of RSCs and SO_2. Detailed descriptions of the target area and RSCs measurements are in Song et al. (2009b).

2.2 Study Approach

The effects of ventilation and photochemical oxidation of RSCs and/or SO_2 on SO_2 concentration levels in the study area were assessed by two sets of simulation scenarios: (1) high (HV) and (2) low ventilation (LV) conditions. For the purpose of this study, two periods (21 October 2008 for the HV case and 16 October 2008 for the LV case) were selected. Under HV, strong easterly and northeasterly winds (up to 5 m s^{-1}) with moderate cloud cover during early morning hours [e.g., 0700 - 1000 local standard time (LST)] were observed. In contrast, with LV, conditions were characterized by a high-pressure system with relatively weak winds (≤ 1.3 m s^{-1}). Throughout this study, the model estimates of SO_2 with (TOTAL case) and without (BASE case) photochemical oxidation of the RSCs for the HV and LV conditions were referred to as TOTAL_HV and BASE_HV cases and TOTAL_LV and BASE_LV cases, respectively. The emission concentrations of RSCs for the LV case (on 16 October) were not measured due to restrictions on field observation inside the factories. To compare the relative contribution of photochemical oxidation of RSCs to SO_2 concentrations between HV and LV conditions, RSC emissions for the LV case were assumed to be the same ones as the HV case (on 21 October). A conceptual flow chart indicating the SO_2 production or changes in SO_2 concentrations under the simulation scenarios resulting from various sources and/or processes (e.g., photochemical production, horizontal and vertical advection, etc.) is shown in Fig. 2.

To compare ventilation conditions between the two different simulation scenarios in the target area, the ventilation rate [or ventilation coefficient (VC)] was estimated using the Penn State/NCAR meteorological model (MM5, Grell

et al. 1994). In general, the VC (m^2 s^{-1})[= h (m) × $\overline{U}$ (m s^{-1})] below the planetary boundary layer (PBL) can be defined as the product of the mixing height (MH, h) and the wind speed ($\overline{U}$), simulated by the MM5, vertically averaged over the mixing layer during morning hours (e.g., 0700 - 1000 LST)(Athanassiadis et al. 2002). Table 1 provides the comparison of VCs between HV and LV conditions (from 0700 to 1000 LST). For the HV condition, the VC was 728 m^2 s^{-1} at 0900 LST and increased to 2456 m^2 s^{-1} at 1000 LST. With LV condition, the VCs at 0900 (77 m^2 s^{-1}) and 1000 LST (724 m^2 s^{-1}) were 10 and 3 times lower than those with HV, respectively. The VCs at 0700 and 0800 LST were not estimated because the MHs simulated by the MM5 at the same time were below the lowest layer (i.e., < 20 m) within

the model (i.e., MM5), regardless of ventilation conditions. Therefore, the ratio of VCs for the HV condition to VCs for the LV condition at 0700 and 0800 LST were excluded from the comparison analysis due to the large uncertainties.

A comparison between observed and predicted values such as meteorological variables (wind speed and direction and air temperature) and SO_2 concentrations for the model validation was conducted for HV and LV conditions in the study area. The meteorological sites were located in Nambu (M1: about 5 km away from EG IC) and Ungsang (M2: about 2 km away from US IC)(Fig. 1). The air quality (including SO_2) monitoring sites (A1 and A2) were located less than 1 km away from the meteorological monitoring sites (Fig. 1).
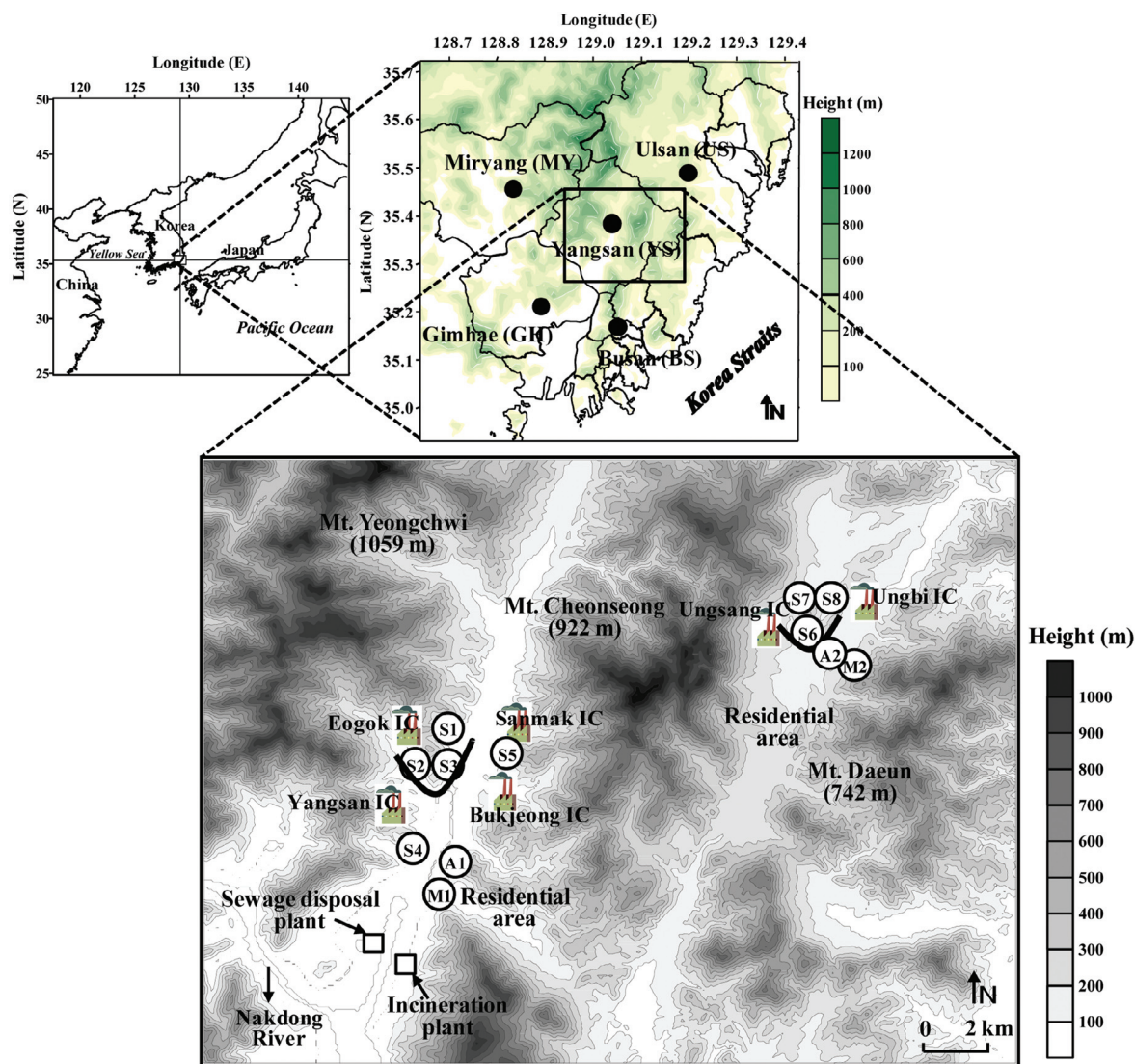

Fig. 1. Schematic diagram of the study area including 8 sampling sites (S1 - S8) for four RSCs and two meteorological (M1 and M2) and two air quality (including SO_2) monitoring sites (A1 and A2) in Yangsan (35°16' - 35°32'N and 128°52' - 129°08'E). Individual sampling locations of the study area are assigned as: (1) S1 - S3 = tire plants; (2) S4 = waste water disposal plant; (3) S5 = oil refinery; (4) S6 = paper mill and incineration plant; and (5) S7 - S8 = livestock feedlots. M1 and M2 indicate the meteorological monitoring sites (M1: Nambu and M2: Ungsang). The sites A1 and A2 are located less than 1 km away from the meteorological sites. The symbol "V" denotes the valley topography in the study area.
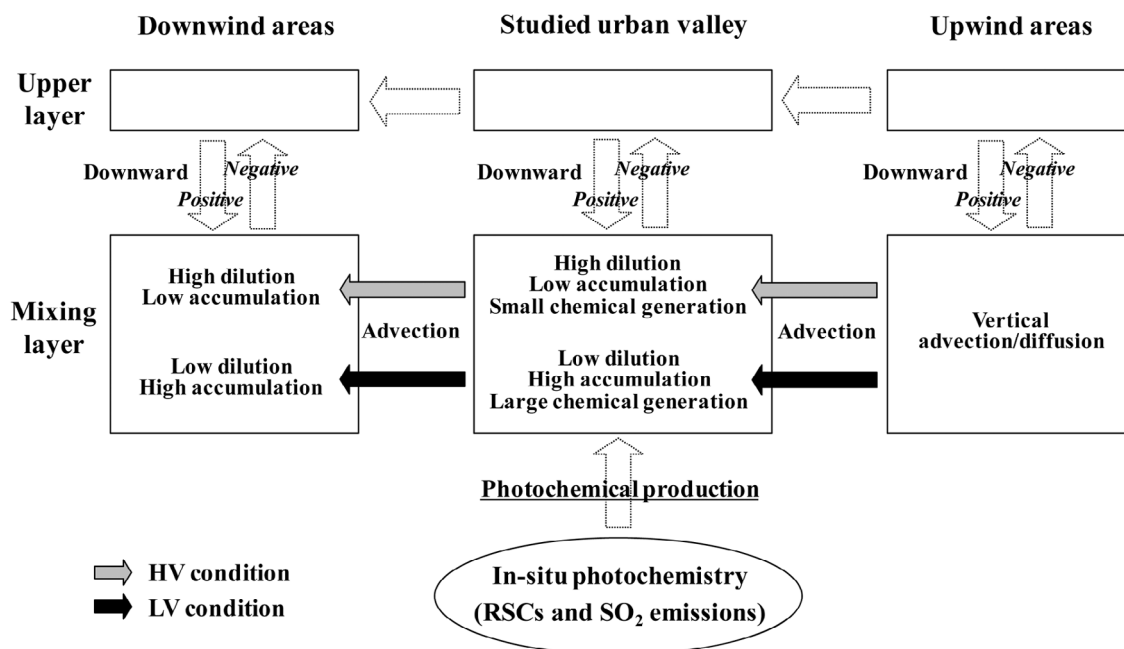
Fig. 2. Conceptual flow chart indicating the SO$_2$ production/concentrations change resulting from various sources and/or processes under the different ventilation conditions (i.e., the HV and LV conditions).

Table 1. Comparison of VCs over the mixing layer calculated from 0700 to 1000 LST between HV (21 October 2008) and LV conditions (16 October 2008) in the study area.

Time (LST)	HV condition			LV condition			VC$_{HV}$/VC$_{LV}$ [b]
	h (m)	$\overline{U}$ (m s^{-1})	VC [a] (m^2 s^{-1})	h (m)	$\overline{U}$ (m s^{-1})	VC (m^2 s^{-1})	
7:00	L*	-**	-	L	-	-	-
8:00	L	-	-	L	-	-	-
9:00	242.5	3.0	727.5	128.9	0.6	77.3	9.4
10:00	501.2	4.9	2455.9	557.0	1.3	724.1	3.4

[a] VC can be defined as a product of the MH (h) and the wind speed ($\overline{U}$) vertically averaged over the mixing layer, estimated from the MM5 during the early morning hours (0700 - 1000 LST).

[b] VC$_{HV}$/VC$_{LV}$ denotes the ratio of VC for the HV condition to VC for the LV condition.

* L represents the height below the lowest layer (< 20 m) simulated by the MM5.

** - = not available.

For numerical modeling, the abbreviated oxidation mechanisms of RSCs and the emission rates of RSCs and SO$_2$ were added to the chemical transformation codes. A detailed description of the oxidation mechanisms of RSCs for the estimates of SO$_2$ concentrations is in Shon et al. 2005. In brief, H$_2$S is oxidized by hydroxyl (OH) radical during the day, while CH$_3$SH is oxidized by OH radical during the day, producing CH$_3$S (an SO$_2$ precursor), and by nitrate (NO$_3$) radical at night. DMS oxidation by OH and NO$_3$ is suggested to proceed by two mechanisms: addition and abstraction channels for OH oxidation, and the abstraction channel for

NO$_3$ oxidation. Like DMS, DMDS can be oxidized by OH to form CH$_3$S and CH$_3$SOH and by NO$_3$ to form CH$_3$S and CH$_3$SO. In addition, the SO$_2$ concentrations in the source and surrounding regions were estimated by considering both the chemical transformation (and ventilation conditions) of the RSCs and the emissions/ventilation of SO$_2$. The spatial distributions of SO$_2$ were estimated among five different regions [Yangsan (YS), Miryang (MY), Gimhae (GH), Ulsan (US), and Busan (BS)]. The contribution of RSC oxidation to SO$_2$ concentration levels in the source region was also compared with HV and LV.

3. MODEL DESCRIPTION AND STATISTICAL METHOD

3.1 Model Description and Input Data

To evaluate the effects of ventilation and photochemistry of RSCs on SO_2 concentration levels, the mechanisms of chemical transformations of four RSCs for the two different ventilation conditions (HV and LV) were applied to the CALPUFF model (with RIVAD/ARM3 chemical scheme; Morris et al. 1988). The model has three main components: CALMET (meteorological model), CALPUFF (transport and dispersion model), and CALPOST (post processor)(Earth Tech. Inc. 2000). The RIVAD/ARM3 chemical scheme includes the conversion processes between NO and NO_2, transformation processes of NO_2 (to total nitrate) and SO_2 (to sulfate), and estimates of major RSC oxidants (e.g., OH and NO_3 radicals). Detailed information on the chemical processes (e.g., oxidation mechanisms of RSCs, estimates of radical concentrations, and photochemical loss frequency of SO_2) in the CALPUFF model was reported previously (Song et al. 2008).

The MM5 was used to simulate the initial conditions for CALMET. The computational domain in MM5 consisted of 23 sigma vertical levels and 38×40 grid points in a horizontal grid size with a resolution of 81 km (center at 37.3°N, 126.3°E). The entire study area was assigned five domains using the one-way nesting method. The smallest domain included 88×88 km grid points with a resolution of 1 km to cover 34.9 to 35.7°N and 128.7 to 129.4°E (Fig. 1). The MM5 physical options used for the simulations were the Grell cumulus scheme, MRF PBL scheme, Dudhia simple-ice moisture scheme, the RRTM long-wave scheme, and the Noah land surface model. The MM5 simulations were carried out using 23-category land-use data from Environmental Geographic Information System (EGIS) to reflect the surface conditions of the target area more effectively (http://egis.me.go.kr/egis/). The initial and lateral boundary conditions were generated every 6 h by interpolating the National Center for Environmental Prediction (NCEP)-FNL model analysis fields with 1-degree resolution at the standard pressure levels. A time step of 120 s was employed for each of two individual durations: (1) an 81-h period [from 0000 Universal Time Coordinated (UTC) on 20 October to 0900 UTC on 23 October 2008] for the HV condition and (2) an 81-h period (from 0000 UTC on 14 October to 0900 UTC on 17 October 2008) for the LV condition.

The emission rate for each of the four RSCs was calculated with emission concentrations and exit velocity at the eight sampling sites and was then used as input data for the CALPUFF model. The point sources of four RSCs were aggregated into the 1×1 km CALPUFF grids, and their emission rates were assigned to eight grid locations in the model domain. SO_2 emission rates were also used for the CALPUFF model to assess SO_2 concentrations along the downwind direction from source regions. The point and area sources of SO_2 were estimated using the Clean Air Policy Support System (CAPSS) provided by the National Institute of Environmental Research (NIER), Korea. Detailed information on the CAPSS for SO_2 emissions is in Song et al. (2008).

Emission rates for RSCs and SO_2 were converted to daily emissions and then the derived daily emission rates were converted to hourly ones. To convert daily to hourly emission rates for RSCs and SO_2, the 24-h temporal assignment factors (range of 0.012 to 0.061) were applied using the Emissions Modeling Clearinghouse (EMCH) model (http://www.epa.gov/ttn/chief/emch/temporal/). The hourly mean emission rates for the four RSCs and stack characteristics at the eight sources are listed in Table 2. The estimated emission rates for H_2S, CH_3SH, DMS, and DMDS ranged from 1.1 (S8) to 28.5 (S1), < 0.01 (S3 - S4 and S7 - S8) to 15.5 (S1), < 0.01 (S4 - S6) to 22.3 (S1), and < 0.01 (S4 and S6 - S8) to 27.4 (S1) g s^{-1} with medians of 7.0 (a mean of 10.7), 0.6 (3.6), 0.6 (5.7), and 0.01 (3.4) g s^{-1}, respectively. The largest SO_2 point and area sources had the emission rates of 3.6×10^0 (a median of 2.4×10^{-4}) and 3.6×10^{-6} (6.4×10^{-8}) g s^{-1}, respectively.

3.2 Statistical Analysis

To assess the accuracies between the observed and predicted values such as meteorological variables (wind speed and direction and air temperature) and SO_2 concentrations, the mean, deviation, Root Mean Square Error (RMSE), and Index Of Agreement (IOA) were calculated. For the calculation of two statistics (RMSE and IOA), the threshold value for wind direction was set to the wind speed of the corresponding data points because the wind direction has no meaning under calm conditions. Therefore, data for wind direction corresponding to an observed wind speed exceeding 0.5 m s^{-1} were used in the statistical analysis. Note that the IOA for wind direction was expressed semi-quantitatively with dominant wind direction. The RMSE and IOA can be expressed as follows:

$$RMSE = \left[\frac{1}{N} \sum_{i=1}^{N} (P_i - O_i)^2 \right]^{1/2} \qquad (1)$$

$$IOA = 1 - \left[\frac{\sum_{i=1}^{N} (P_i - O_i)^2}{\sum_{i=1}^{N} (|P_i - M_o| + |O_i - M_o|)^2} \right] \qquad (2)$$

where P_i and O_i are the predicted and observed values of variable i, respectively; N is the total number of observations; and M_o is the average value of the observation. An IOA of 1 indicates perfect agreement between the predicted

and observed data, while an IOA of zero denotes no agreement at all.

4. RESULTS AND DISCUSSION

4.1 Statistical Evaluation of Meteorological Variables and SO₂ Concentrations

Table 3 shows the IOA and RMSE of the meteorological variables and SO₂ concentrations with HV and LV at M1 and M2 for the meteorological variables and A1 and A2 for the SO₂ (Fig. 1). Overall, most of the IOAs of wind speed and air temperature were greater than 0.6, regardless of sites and ventilation conditions. The maximum IOAs of the wind speed and air temperature reached 0.89 and 0.81 at sites M1 and M2, respectively, with LV. On the other hand, the IOA for SO₂ concentration ranged from 0.51 (at site A1 with HV) to 0.62 (at site A2 with LV). The relatively low IOAs of SO₂ concentration might be due to the lack of information concerning RSCs and SO₂ emission outside the industrial sources (S1 - S8) in the study area. The RMSEs of meteorological variables were less than 1.3 m s^{-1} for the wind speed, less than 79° for the wind direction, and less than

Table 2. Stack emission characteristics for four RSCs at eight CALPUFF grid locations in the model domain.

Grid No.	Longitude (°E)	Latitude (°N)	Stack height (m)	Stack inner diameter (m)	Exit temp. (K)	Exit velocity (m s^{-1})	Emission rates (g s^{-1}) [a]			
							H₂S	CH₃SH	DMS	DMDS
1	129.05	35.37	12.3	0.8	307.6	19.7	28.52	15.54	22.30	27.40
2	129.04	35.36	17.0	1.9	311.0	3.9	12.05	7.88	4.97	0.01
3	129.05	35.36	13.8	1.4	408.0	19.0	26.20	< 0.01	16.96	0.03
4	129.04	35.34	15.0	15.0	420.0	7.9	3.41	< 0.01	< 0.01	< 0.01
5	129.06	35.37	78.5	2.4	453.7	6.7	10.58	4.07	< 0.01	0.01
6	129.16	35.41	11.5	1.6	403.0	18.0	2.56	1.11	< 0.01	< 0.01
7	129.16	35.42	10.0	15.0	297.3	3.9	1.52	< 0.01	0.64	< 0.01
8	129.17	35.42	10.0	15.0	297.3	3.9	1.13	< 0.01	0.59	< 0.01

[a] *The hourly mean emission rate for each of the four RSCs was determined by emission concentrations and exit velocity in the emission sources.*

Table 3. Statistical evaluation between observed and predicted meteorological variables and SO₂ concentrations for the HV and LV conditions at two monitoring sites in Yangsan during the study period (20 - 22 October 2008 for the HV condition and 15 - 17 October 2008 for the LV condition).

Ventilation condition	Meteorological and SO₂ data sites [*]	Wind speed		Wind direction		Air temperature		SO₂	
		IOA [a]	RMSE [b]	Dominant wind direction	RMSE	IOA	RMSE	IOA	RMSE
HV Condition	Nambu	0.592	1.103	NNW/NE [c]	78.630	0.678	3.239	0.508	29.640
	Ungsang	0.799	1.266	N/NE	68.035	0.686	3.141	0.548	39.950
LV Condition	Nambu	0.619	1.125	NE/E	74.142	0.891	2.747	0.535	33.273
	Ungsang	0.802	0.756	E/NE	67.392	0.810	3.451	0.616	34.144
DIFF**		+0.015	-0.244		-2.566	+0.169	-0.091	+0.048	-1.087

[a] *IOA: index of agreement.*

[b] *RMSE: root mean square error.*

[c] *The observed/modeled values of dominant wind direction.*

[*] *Nambu and Ungsang sites represent the meteorological monitoring sites as shown in Fig. 1. The SO₂ measurement sites were located less than 1 km away from the meteorological sites.*

** *The difference in the simulated values between the HV and LV cases (LV-HV). The positive and negative values signify that the values are larger and smaller in the LV condition than those in the HV condition, respectively.*

3.5°C for the air temperature. In addition, the differences in the IOAs of wind speed (+0.015), air temperature (+0.169), and SO_2 concentration (+0.048) between the two ventilation conditions were found to be positive, while those of the RMSEs of wind speed (-0.244), wind direction (-2.566), air temperature (-0.091), and SO_2 concentration (-1.087) were negative. This suggests that the accuracy of the wind speed, air temperature, and SO_2 concentration tended to be slightly higher with LV than with HV.

These values of IOAs and RMSEs for the meteorological variables were similar to those reported in the literature associated with other applications of mesoscale models (e.g., MM5). Previous studies found IOAs for wind speed and air temperature ranging from 0.29 to 0.78 m s^{-1} (Papalexiou and Moussiopoulos 2006) and from 0.82 to 0.94°C (Lee and Fernando 2004; Papalexiou and Moussiopoulos 2006), respectively. RMSEs for wind speed and

direction and air temperature ranged from 0.65 to 1.69 m s^{-1} (Papalexiou and Moussiopoulos 2006), from 25 to 102° (Papalexiou and Moussiopoulos 2006), from 1.94 to 2.94°C (Seaman and Michelson 2000), respectively. Therefore, the results of this study indicate that the simulations of these experimental scenarios might be reasonable for assessing the influence of meteorological conditions (e.g., ventilation) on SO_2 concentrations.

4.2 Effects of Ventilation and Photochemical Oxidation of RSCs on SO_2 Formation

Figure 3 shows the SO_2 concentrations simulated at 0900 and 1500 LST for the TOTAL_HV and TOTAL_LV cases. Overall, the SO_2 concentrations in the surface layer depended largely on the wind speed and direction (mostly easterly and northerly winds) of the air inflow. Strong
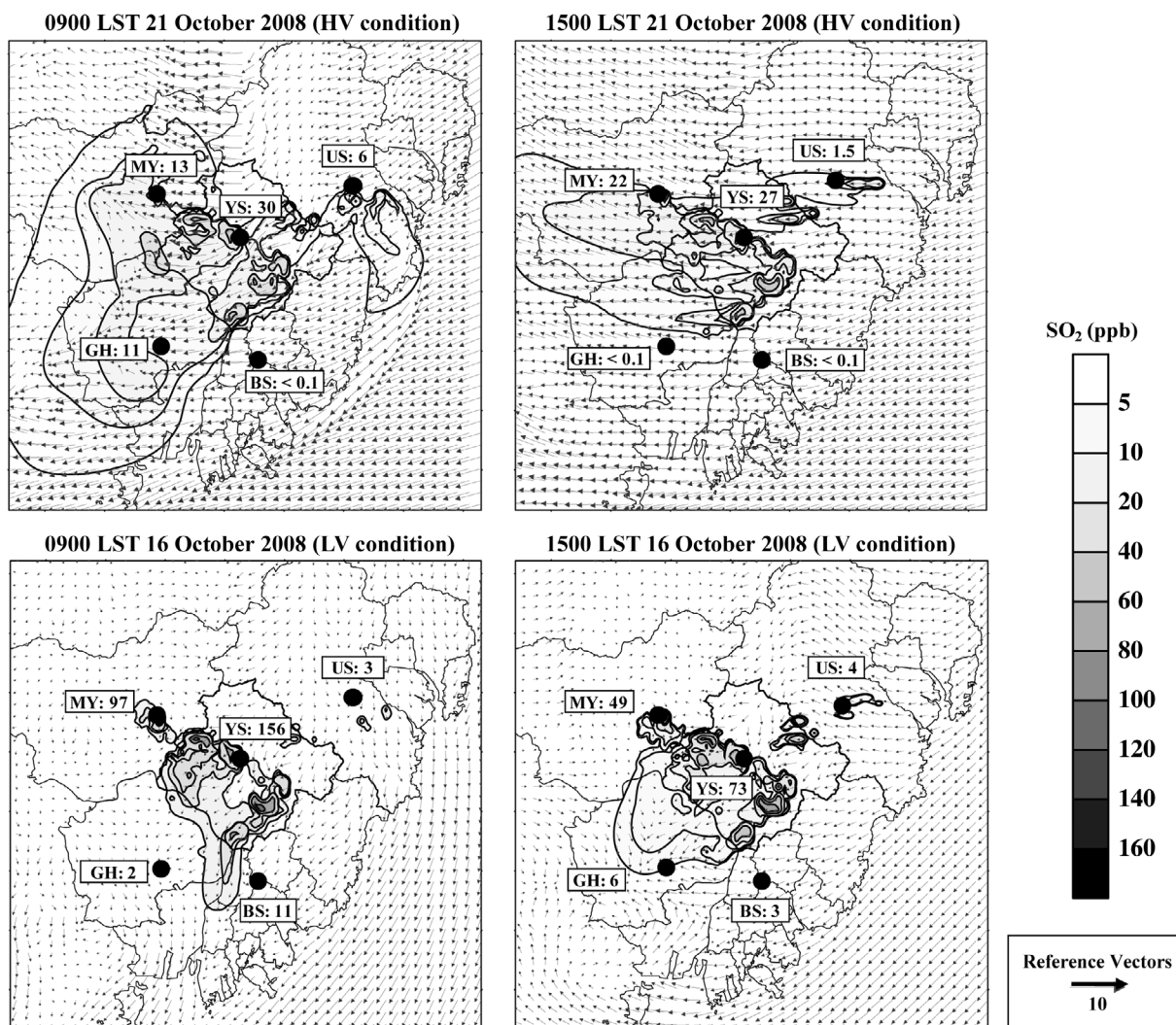

Fig. 3. Horizontal distributions of the simulated wind vectors (m s^{-1}) and SO_2 concentrations (ppb) at 0900 and 1500 LST for the TOTAL_HV and TOTAL_LV cases, respectively. The values within the rectangles indicate simulated SO_2 concentrations in the five regions (including the target industrial source regions in YS).

winds ($\geq$ 5 m s^{-1}) were prominent in the TOTAL_HV case, whereas relatively weak local winds (range of 0.1 - 5 m s^{-1}) were dominant in the TOTAL_LV case. The temporal and spatial distributions of SO$_2$ in the study area were significantly different between the two cases. For the TOTAL_HV case, SO$_2$ concentrations below 30 ppb at both 0900 and 1500 LST were estimated from the industrial area (in YS) to downwind regions (e.g., MY and GH located at more than 10 km west and southwest of YS, respectively) due to the dispersion by the strong easterly winds ($\geq$ 5 m s^{-1}). On the other hand, SO$_2$ concentrations in US and BS were relatively lower ($\leq$ 6 ppb).

Vertical and/or horizontal dispersion between the source and downwind regions can affect the distributions of SO$_2$ in the target study area, YS. For the TOTAL_HV case, the SO$_2$ concentrations in the surrounding/downwind regions of YS (e.g., MY and GH) at 0900 LST on 21 October might have been affected by the vertical and/or horizontal advection of SO$_2$ trapped within the mixing layer (about 1000 - 1700 m, not shown) in the afternoon on the day before (20 October) in the source regions of YS. At 1500 LST on 21 October, SO$_2$ concentrations in the downwind regions of YS might result from the combined effect such as dispersion from YS to its downwind regions (due to higher MHs in the afternoon than the surrounding mountainous elevation) and photochemical oxidation of RSCs and/or SO$_2$.

For the TOTAL_LV case, SO$_2$ concentrations in the source regions of YS were considerably higher than those of the other areas (MY, GH, US, and BS) regardless of time. In the morning (e.g., 0900 LST), significantly high SO$_2$ concentrations (e.g., 156 ppb) were estimated in the industrial source regions due both to very weak winds ($\leq$ 1.3 m s^{-1}) and low MHs (< 130 m at 0900 LST), as shown in Table 1. This may result from stagnation of air masses under the LV condition with the low VC of 77 m^2 s^{-1} (up to 9 times lower than those of the HV condition) in the morning (Table 1). Although northerly winds (from YS to BS) were dominant in this case, the SO$_2$ contributions of YS source regions to SO$_2$ levels in BS in the afternoon (e.g., 1500 LST) were relatively small due in part to the enhanced dilution in comparison with that in the morning.

A comparison of SO$_2$ concentrations between the TOTAL (TOTAL_HV and TOTAL_LV) and BASE cases (BASE_HV and BASE_LV) under different ventilation conditions indicates that considerable quantities of SO$_2$ on 16 October can be produced in the source regions due to the ventilation effect during the early morning and daytime photochemistry. Note that the early morning is defined as the time when the ventilation rate is high (0700 - 1000 LST, Athanassiadis et al. 2002) and the daytime as the time when photochemical reactions are active (0600 - 1800 LST). Table 4 shows the simulated SO$_2$ concentrations for TOTAL_HV and TOTAL_LV and without photochemical oxidation of the four RSCs (BASE_HV and BASE_LV)

in the target source region (YS) and its downwind regions (e.g., MY and BS) during the study period. For comparison of modeled SO$_2$ in different regions, two pairs of three cities (e.g., YS, MY, and BS) were selected: (1) YS and MY (for HV) and (2) YS and BS (for LV), based on the analysis of airflow patterns shown in Fig. 3.

In the source region (YS), SO$_2$ estimates for the TOTAL_HV case [a mean of 6.3 (during the early morning) and 5.0 ppb (during the daytime)] were found to be approximately an order of magnitude lower than those of the TOTAL_LV case (64 and 40 ppb)(Table 4). In the downwind region, the former pair (4.2 and 3.4 ppb) was found to be about a factor of 3 lower than the latter (13 and 8 ppb). SO$_2$ estimates in YS for the BASE_HV case (a mean of 3.0 during the early morning and 2.9 ppb during the daytime) were found to be about a factor of 3 lower than those for the BASE_LV case (8.9 and 7.8 ppb)(Table 4). In the downwind region, BASE_HV concentrations (3.0 and 2.8 ppb) were about a factor of 1.3 lower than BASE_LV (4.0 and 3.3 ppb).

During the daytime, the mean values of newly generated (TOTAL-BASE, range of 20 - 90 ppb) and advected SO$_2$ concentrations (BASE case, ~20 ppb in the early morning) at some sites in the source region (e.g., EG IC) with LV were considerably higher than those ($\leq$ 2 and $\leq$ 5 ppb, respectively) with HV (Fig. 4). The relatively high advected SO$_2$ concentrations with LV during the early morning (0700

Table 4. Simulated SO$_2$ concentrations for TOTAL (TOTAL_HV and TOTAL_LV) and BASE cases (BASE_HV and BASE_LV) with HV and LV in Yangsan and downwind regions (MY and BS)(in ppb).

Ventilation condition	Area *	[SO$_2$]$_{BASE}$	[SO$_2$]$_{TOTAL}$
		[SO$_2$]$_{BASE\_HV}$	[SO$_2$]$_{TOTAL\_HV}$
HV	YS	3.0[a] (2.9)[b]	6.3 (5.0)
condition	MY	3.0 (2.8)	4.2 (3.4)
		[SO$_2$]$_{BASE\_LV}$	[SO$_2$]$_{TOTAL\_LV}$
LV	YS	8.9 (7.8)	64.4 (39.7)
condition	BS	4.0 (3.3)	13.3 (7.7)
LV/HV[c]	YS	3.0 (2.7)	10.2 (7.9)
	MY or BS	1.3 (1.2)	3.2 (2.3)

[a] Mean SO$_2$ concentrations simulated during the early morning (0700 - 1000 LST).
[b] Mean SO$_2$ concentrations simulated during the daytime (0600 - 1800 LST).
[c] LV/HV denotes [SO$_2$]$_{BASE\_LV}$/[SO$_2$]$_{BASE\_HV}$ and [SO$_2$]$_{TOTAL\_LV}$/[SO$_2$]$_{TOTAL\_HV}$ for the HV and LV conditions between the TOTAL and BASE cases in YS and its downwind regions, respectively.
* YS: Yangsan; MY: Miryang; BS: Busan.

- 0800 LST) were likely the result of positive contributions of vertically downward movement from the upper layer and in part from the horizontal advection from the upwind source site (e.g., site S4 located 3 - 4 km south of EG IC,

Fig. 1) along southerly winds (Fig. 4). Despite the strong winds (northeasterly winds shown in Fig. 4) with HV, the SO_2 concentrations advected from upwind sites were considerably lower because of lack of emission sources at upwind
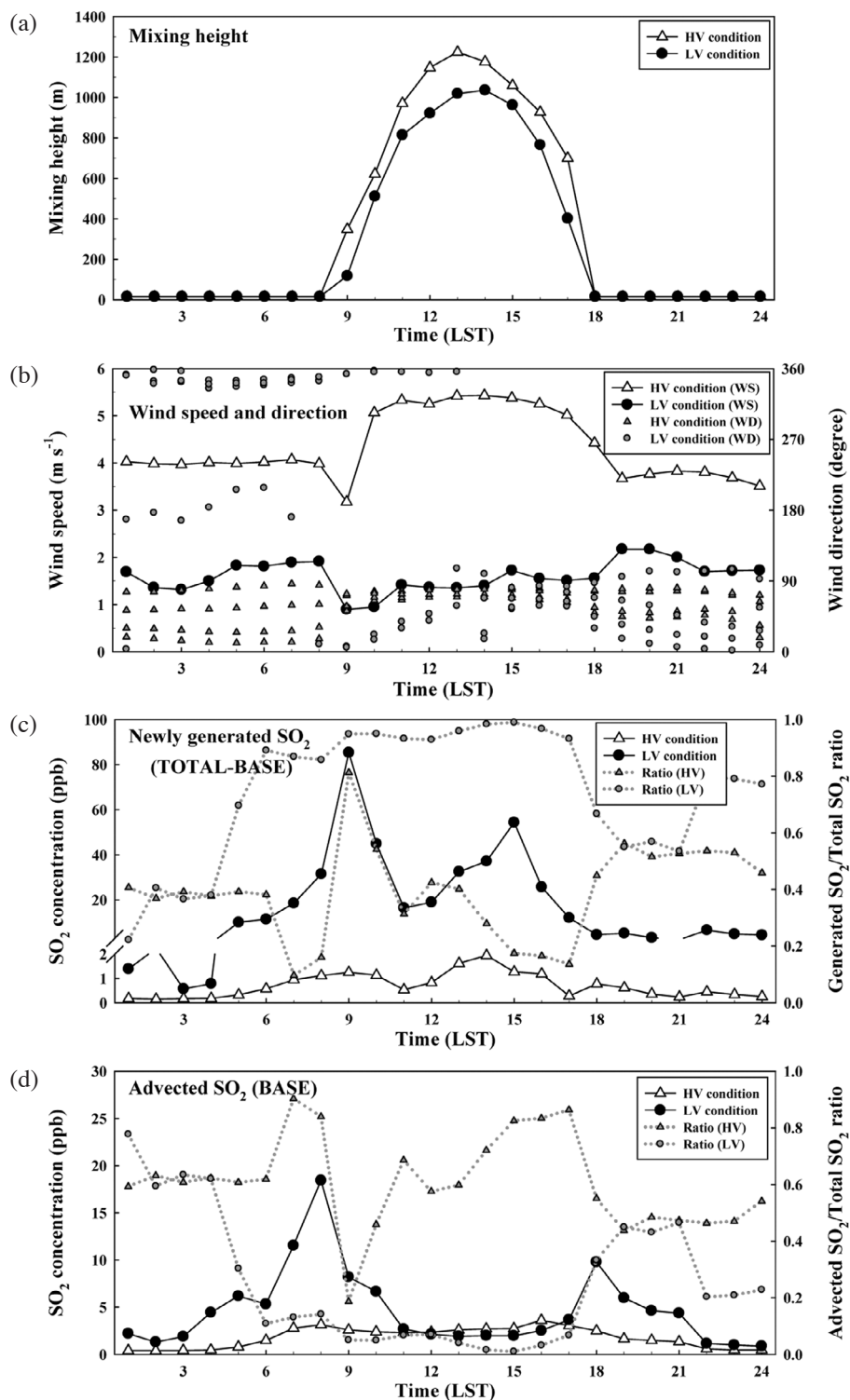

Fig. 4. Diurnal variations of the (a) mixing height, (b) wind speed and direction, (c) newly generated SO_2 (TOTAL-BASE), and (d) advected SO_2 (BASE case) for the HV and LV conditions at several sites in the source region (e.g., EG IC) of YS. The thin dotted lines in lower two panels represent the ratios of newly generated and advected SO_2 to total SO_2 concentrations for the HV (···△···) and LV conditions (···●···), respectively.

sites (a residential area) located northeast from EG IC. Meanwhile, despite low photochemical activities in the morning, the increase in newly generated SO_2 concentrations might have been mainly caused by the photochemical oxidation of accumulated RSCs due to the low ventilation effect (e.g., VC_{HV}/VC_{LV} ratio of 9.4, the wind speed of about 1 m s^{-1}, Table 1) with low MHs (< 600 m) in the morning and in part by high temporal assignment factors (0.061) for RSC emissions in the daytime (morning and afternoon). The sharp decrease in wind speed at 0900 LST under the two conditions might be related to change in wind direction (NE → E for the HV condition and N or S → E for the LV condition).

To thoroughly evaluate the relative contribution between ventilation and photochemical conversion of RSCs and/or SO_2 to SO_2 production, the ratios of the newly generated and advected SO_2 to total SO_2 concentrations were compared between HV and LV, respectively (Fig. 4). Overall, the ratios of newly generated and advected SO_2 to total SO_2 concentrations during the daytime were estimated to be 0.3 and 0.7 for HV and 0.9 and 0.1 for LV, respectively. Compared with HV, the ratio of newly generated SO_2 to total SO_2 concentrations for LV was significantly higher. However, the ratio of advected SO_2 to total SO_2 concentrations for the HV condition was significantly higher (a factor of 7 during the daytime) than that for the LV condition. This implies that the photochemical conversion of RSCs to SO_2 with LV can be a very important source rather than advection and vice versa for HV.

For the TOTAL case, significantly higher SO_2 concentration ratios (range of 7.9 - 10.2) of the LV condition to the HV condition (= $[SO_2]_{TOTAL\_LV}/[SO_2]_{TOTAL\_HV}$) in YS than the ratios (2.3 - 3.2) in the downwind region indicated that SO_2 concentrations in YS were strongly impacted by the ventilation condition of RSCs and SO_2 and photochemical oxidation of RSCs. Compared to the TOTAL case, for the BASE case (Table 4), slightly higher $[SO_2]_{BASE\_LV}/[SO_2]_{BASE\_HV}$ ratio (range of 2.7 - 3.0) in YS than the ratios (1.2 - 1.3) in the downwind region implies that photochemical oxidation of RSCs to SO_2 played a significant role in determining the pattern in SO_2 concentrations.

4.3 Contribution of RSC Oxidation to SO_2 Concentrations with HV and LV

The relative contributions of photochemical oxidation of individual RSCs to SO_2 formation averaged from 8 grid locations (or 8 industrial sources) in YS were compared under the two ventilation conditions during the early morning and the daytime (Fig. 5). The photochemical production of SO_2 (TOTAL - BASE) was highly variable between HV and LV: 27% of total SO_2 concentrations (during the early morning) and 16% (during the daytime) for HV and 78% (during the early morning) and 69% (during the daytime) for LV. The estimated SO_2 due to photochemical oxidation

of RSCs in the HV case was similar to that estimated in our previous studies performed during the fall around a Korean industrial complex (approximately 20%)(Song et al. 2008) and around a coastal landfill (21%)(Song et al. 2009a). The fractions for LV were significantly higher than those found for the two previous studies. We also found strong diurnal variations in the contribution of RSCs (to SO_2 formation) from case to case. The SO_2 concentrations formed by oxidative conversion of individual RSCs for the HV condition ($[SO_2]_{TOTAL\_HV}$ - $[SO_2]_{BASE\_HV}$) were found to be 1.3 (range of 0.02 - 0.91 ppb) for S1 - S8 during the early morning and 0.7 ppb (0.02 - 0.42 ppb) during the daytime, whereas those for the LV condition were 46.5 (0.26 - 37.6 ppb) and 24.6 (0.14 - 19.9 ppb), respectively. The difference in photochemical SO_2 formation between two time periods under the two ventilation conditions might be primarily caused by the combination of photochemical reactivity and the difference in ventilation effects of RSCs and SO_2 emitted from the source region (YS).

Photochemical production of SO_2 in all cases was generally dominated by DMDS, H_2S, or CH_3SH. The fraction of individual RSCs contributing to total photochemical SO_2 formation under the HV condition (TOTAL_HV - BASE_HV) was estimated to be approximately 73% for DMDS and 17% for CH_3SH during the early morning and 61% for DMDS, 19% for H_2S, or 18% for CH_3SH during the daytime (Fig. 5). Contributions from DMS were a minor component of RSCs to the formation of SO_2, with fractions ranging from 2 - 3% of the total SO_2 concentrations. For the SO_2 concentration newly generated from RSC oxidation for the LV condition (TOTAL_LV - BASE_LV), DMDS was a dominant contributor (81%) followed by CH_3SH (13%), H_2S (5%), and DMS (1%) during both the early morning and the daytime (Fig. 5). This might be primarily caused by higher photochemical reactivity for DMDS oxidation compared with the other RSCs (e.g., H_2S, CH_3SH, and DMS). For instance, the rate constant (about 2.4 × 10^{-10} cm^3 molec^{-1} s^{-1} at a mean temperature of 293 K) for DMDS was significantly higher than those [range of 4.7 × 10^{-12} (H_2S) to 3.4 × 10^{-11} (CH_3SH)] for the other RSCs. Therefore, evaluation of the relative contributions between different RSCs regardless of ventilation conditions indicated that SO_2 formation was most sensitively influenced by DMDS. When the relative contribution of photochemical conversion in the urban valley (Yangsan) was compared with other regions, the results shown here are similar to those in previous studies, suggesting that DMDS played a leading role in SO_2 formation in an urban center (Shon and Kim 2006) as well as a landfill area (Song et al. 2007).

5. SUMMARY AND CONCLUSIONS

Temporal and spatial distributions of simulated SO_2 concentrations were related to changes in the wind direction
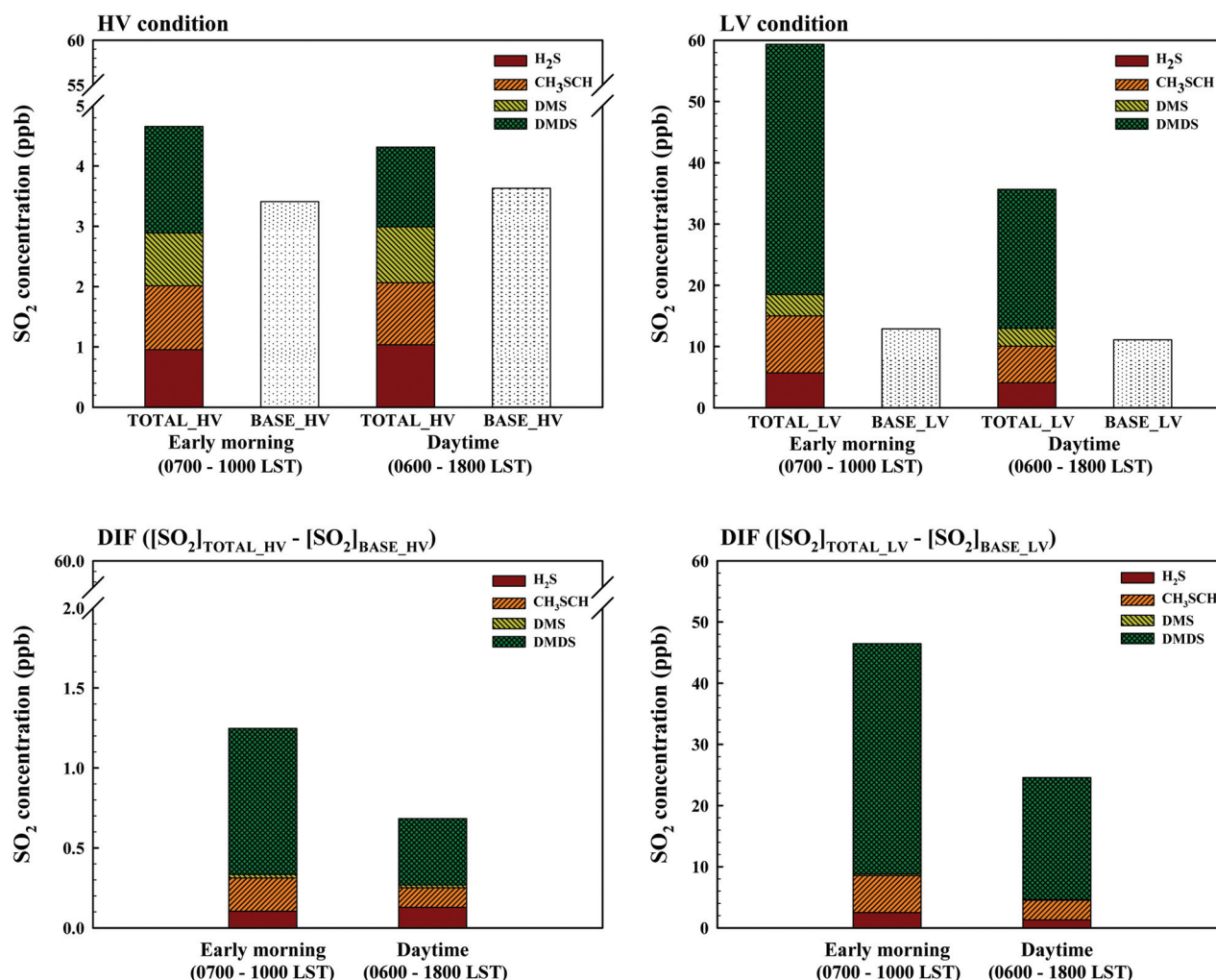
Fig. 5. Relative contribution of photochemical oxidation of individual RSCs to the SO_2 formation averaged from 8 industrial sources (i.e., S1 - S8) within the study domain for HV and LV during the early morning (0700 - 1000 LST) and during the daytime (0600 - 1800 LST). DIF denotes the difference of SO_2 concentrations between the TOTAL and BASE cases (TOTAL-BASE) for the HV and LV conditions.

and speed of the air flows. Our results showed that moderately low SO_2 concentrations ($\leq$ 30 ppb) with HV (TOTAL_HV case) were predicted in the target source (in YS) and its surrounding regions (at both 0900 and 1500 LST) due to the dispersion along the strong synoptic-scale winds ($>$ 5 m s^{-1}). In contrast, higher SO_2 concentrations (up to 156 ppb at 0900 LST) with LV (TOTAL_LV case) were predicted in and around the target source region. This may have been caused by the photochemical conversion of RSCs and accumulation of RSCs and SO_2 with LV as a result of weak winds (about 1 m s^{-1}), low MHs ($<$ 130 m at 0900 LST), and considerably lower VCs in the morning. Moreover, the simulated meteorological variables showed fair agreement with those of the observations [the maximum IOAs for wind speed (0.80) and air temperature (0.89), and RMSEs of $\leq$ 1.3 m s^{-1} for wind speed, $\leq$ 79° for wind direction, and $\leq$ 3.5°C for air temperature].

The photochemical production of SO_2 with LV (TO-

TAL_LV - BASE_LV)(up to 78% of total SO_2 concentrations in the early morning) was remarkably higher than that with HV (TOTAL_HV - BASE_HV)(up to 27%) during the study period. The total photochemical production of SO_2 for the TOTAL_HV case was generally dominated by DMDS (about 73% of total contribution) and CH_3SH (17%) during the early morning and by DMDS (61%) and H_2S (19%) during the daytime. For the TOTAL_LV case, DMDS was also a fairly dominant contributor (81%) regardless of time period, and CH_3SH accounted for 13% of total SO_2 concentrations. Meanwhile, the contribution of the other RSCs (H_2S and DMS) was found to be insignificant (e.g., $\leq$ 5%). Thus, evaluation of the relative contributions of the four RSCs suggests that the formation of SO_2 was influenced most significantly by DMDS with LV. In this study, it is difficult to accurately evaluate the ventilation effect on SO_2 production/ concentrations in the early morning because of the large uncertainties of estimated MHs. If the MH observation is

accurately carried out in further studies, the assessment of ventilation effect on SO_2 production and concentrations can be improved.

REFERENCES

Athanassiadis, G. A., S. T. Rao, J. Y. Ku, and R. D. Clark, 2002: Boundary layer evolution and its influence on ground-level ozone concentrations. *Environ. Fluid Mech.*, **2**, 339-357, doi: 10.1023/A:1020456018087. [Link]

Bates, T. S., B. K. Lamb, A. Guenther, J. Dignon, and R. E. Stoiber, 1992: Sulfur emissions to the atmosphere from natural sources. *J. Atmos. Chem.*, **14**, 315-337, doi: 10.1007/BF00115242. [Link]

Berman, S., J. Y. Ku, and S. T. Rao, 1999: Spatial and temporal variation in the mixing depth over the northeastern United States during the summer of 1995. *J. Appl. Meteorol.*, **38**, 1661-1673, doi: 10.1175/1520-0450(1999)038<1661:SATVIT>2.0.CO;2. [Link]

Blaha, D., K. Bartlett, P. Czepiel, R. Harriss, and P. Crill, 1999: Natural and anthropogenic methane sources in New England. *Atmos. Environ.*, **33**, 243-255, doi: 10.1016/S1352-2310(98)00153-8. [Link]

Davoli, E., M. L. Gangai, L. Morselli, and D. Tonelli, 2003: Characterisation of odorants emissions from landfills by SPME and GC/MS. *Chemosphere*, **51**, 357-368, doi: 10.1016/S0045-6535(02)00845-7. [Link]

Earth Tech. Inc., 2000. A User's Guide for the CALPUFF Dispersion Model Version 5. Concord, MA.

Grell, G. A., J. Dudhia, and D. R. Stauffer, 1994: A description of the fifth-generation Penn State/NCAR Mesoscale Model (MM5)-NCAR/TN-398 + STR., NCAR, Boulder, CO, USA.

Gurjar, B. R., J. A. van Aardenne, J. Lelieveld, and M. Mohan, 2004: Emission estimates and trends (1990-2000) for megacity Delhi and implications. *Atmos. Environ.*, **38**, 5663-5681, doi: 10.1016/j.atmosenv.2004.05.057. [Link]

Ito, A., I. Takahashi, Y. Nagata, K. Chiba, and H. Haraguchi, 2001: Spatial and temporal characteristics of urban atmospheric methane in Nagoya City, Japan: An assessment of the contribution from regional landfills. *Atmos. Environ.*, **35**, 3137-3144, doi: 10.1016/S1352-2310(00)00533-1. [Link]

Kim, K. H., 2006: Emissions of reduced sulfur compounds (RSC) as a landfill gas (LFG): A comparative study of young and old landfill facilities. *Atmos. Environ.*, **40**, 6567-6578, doi: 10.1016/j.atmosenv.2006.05.063. [Link]

Kim, K. H., E. C. Jeon, Y. J. Choi, and Y. S. Koo, 2006: The emission characteristics and the related malodor intensities of gaseous reduced sulfur compounds (RSC) in a large industrial complex. *Atmos. Environ.*, **40**, 4478-4490, doi: 10.1016/j.atmosenv.2006.04.026. [Link]

Lee, S. M. and H. J. S. Fernando, 2004: Evaluation of meteorological models MM5 and HOTMAC using PAFEX-I data. *J. Appl. Meteorol.*, **43**, 1133-1148, doi: 10.1175/1520-0450(2004)043<1133:EOMMMA>2.0.CO;2. [Link]

Lin, X. J., S. Barrington, J. Nicell, D. Choinière, and A. Vézina, 2006: Influence of windbreaks on livestock odour dispersion plume in the field. *Agr. Ecosyst. Environ.*, **116**, 263-272, doi: 10.1016/j.agee.2006.02.014. [Link]

Loizidou, M. and E. G. Kapetanios, 1992: Study on the gaseous emissions from a landfill. *Sci. Total Environ.*, **127**, 201-210, doi: 10.1016/0048-9697(92)90503-K. [Link]

Morris, R. E., R. C. Kessler, S. G. Douglas, K. R. Styles, and G. E. Moore, 1988: Rocky mountain acid deposition model assessment: Acid rain mountain mesoscale model (ARM3). US Environmental Protection Agency, Atmospheric Sciences Research Laboratory, Research Triangle Park, NC.

Muezzinoglu, A., 2003: A study of volatile organic sulfur emissions causing urban odors. *Chemosphere*, **51**, 245-252, doi: 10.1016/S0045-6535(02)00821-4. [Link]

Mussio, P., A. W. Gnyp, and P. F. Henshaw, 2001: A fluctuating plume dispersion model for the prediction of odour-impact frequencies from continuous stationary sources. *Atmos. Environ.*, **35**, 2955-2962, doi: 10.1016/S1352-2310(00)00419-2. [Link]

Papalexiou, S. and N. Moussiopoulos, 2006: Wind flow and photochemical air pollution in Thessaloniki, Greece. Part II: Statistical evaluation of European Zooming Model's simulation results. *Environ. Model. Softw.*, **21**, 1752-1758, doi: 10.1016/j.envsoft.2005.09.004. [Link]

Seaman, N. L. and S. A. Michelson, 2000: Mesoscale meteorological structure of a high-ozone episode during the 1995 NARSTO-Northeast Study. *J. Appl. Meteorol.*, **39**, 384-398, doi: 10.1175/1520-0450(2000)039<0384:MMSOAH>2.0.CO;2. [Link]

Shon, Z. H. and K. H. Kim, 2006: Photochemical oxidation of reduced sulfur compounds in an urban location based on short time monitoring data. *Chemosphere*, **63**, 1859-1869, doi: 10.1016/j.*Chemosphere*.2005.10.021. [Link]

Shon, Z. H., K. H. Kim, E. C. Jeon, M. Y. Kim, Y. K. Kim, and S. K. Song, 2005: Photochemistry of reduced sulfur compounds in a landfill environment. *Atmos. Environ.*, **39**, 4803-4814, doi: 10.1016/j.atmosenv.2005.06.024. [Link]

Smith, S. J., H. Pitcher, and T. M. L. Wigley, 2001: Global

and regional anthropogenic sulfur dioxide emissions. *Global Planet. Change*, **29**, 99-119, doi: 10.1016/S09 21-8181(00)00057-6. [Link]

Song, S. K., Z. H. Shon, K. H. Kim, S. C. Kim, Y. K. Kim, and J. K. Kim, 2007: Monitoring of atmospheric reduced sulfur compounds and their oxidation in two coastal landfill areas. *Atmos. Environ.*, **41**, 974-988, doi: 10.1016/j.atmosenv.2006.09.026. [Link]

Song, S. K., Z. H. Shon, K. H. Kim, Y. K. Kim, and R. Pal, 2008: Dispersion and photochemical oxidation of reduced sulfur compounds in and around a large industrial complex in Korea. *Atmos. Environ.*, **42**, 4269-4279, doi: 10.1016/j.atmosenv.2008.01.015. [Link]

Song, S. K., Z. H. Shon, and K. H. Kim, 2009a: Photochemical oxidation and dispersion of gaseous sulfur compounds from natural and anthropogenic sources around a coastal location. *Atmos. Environ.*, **43**, 3015-3023, doi: 10.1016/j.atmosenv.2008.12.037. [Link]

Song, S. K., Z. H. Shon, Y. K. Kim, C. H. Kim, S. Y. Yoo, and S. H. Park, 2009b: Characteristics of malodor pollutants and aromatic VOCs around an urban valley in Korea. *Environ. Monit. Assess.*, **157**, 259-275, doi:

10.1007/s10661-008-0533-x. [Link]

Stern, D. I., 2006: Reversal of the trend in global anthropogenic sulfur emissions. *Global Environ. Change*, **16**, 207-220, doi: 10.1016/j.gloenvcha.2006.01.001. [Link]

Wargocki, P., Z. Bakó-Biró, G. Clausen, and P. O. Fanger, 2002: Air quality in a simulated office environment as a result of reducing pollution sources and increasing ventilation. *Energ. Buildings*, **34**, 775-783, doi: 10.1016/S0378-7788(02)00096-8. [Link]

Warneke, C., S. A. McKeen, J. A. de Gouw, P. D. Goldan, W. C. Kuster, J. S. Holloway, E. J. Williams, B. M. Lerner, D. D. Parrish, M. Trainer, F. C. Fehsenfeld, S. Kato, E. L. Atlas, A. Baker, and D. R. Blake, 2007: Determination of urban volatile organic compound emission ratios and comparison with an emissions database. *J. Geophys. Res.*, **112**, D10S47, doi: 10.1029/2006JD007930. [Link]

Watts, S. F., 2000: The mass budgets of carbonyl sulfide, dimethyl sulfide, carbon disulfide and hydrogen sulfide. *Atmos. Environ.*, **34**, 761-799, doi: 10.1016/S1352-23 10(99)00342-8. [Link]